Clinical Radiology 74 (2019) 975.e1–975.e9

Contents lists available at ScienceDirect

Clinical Radiology

journal homepage: www.clinicalradiologyonline.net

Hepatobiliary phase hypointense nodule without arterial phase hyperenhancement as a risk factor for late recurrence (>1 year) of hepatocellular carcinoma after surgery

M. Matsuda [a], S. Ichikawa [a,*], M. Matsuda [b,c], H. Amemiya [b], D. Ichikawa [b], H. Onishi [a], U. Motosugi [a]

[a] Department of Radiology, University of Yamanashi, 1110 Shimokato, Chuo-shi, Yamanashi, 409-3898, Japan
[b] First Department of Surgery, University of Yamanashi, 1110 Shimokato, Chuo-shi, Yamanashi, 409-3898, Japan
[c] Fujiyoshida Municipal Medical Center, 6530 Kamiyoshida, Yujiyoshida-shi, Yamanashi, 403-0005, Japan

ARTICLE INFORMATION

Article history:
Received 10 May 2019
Accepted 8 August 2019

AIM: To evaluate the value of magnetic resonance imaging (MRI) features, including liver stiffness measured by magnetic resonance elastography (MRE) and the presence of hepatobiliary phase (HBP) hypointense nodule without arterial phase hyperenhancement (APHE), for predicting late recurrence (>1 year) after surgery for hepatocellular carcinoma (HCC).

MATERIALS AND METHODS: This retrospective study included 124 consecutive patients who had undergone surgery for HCC and preoperative MRI. After excluding patients with early recurrence within 1 year after surgery, 89 patients were analysed. Preoperative MRI images were reviewed by a radiologist to record imaging findings, including (1) liver stiffness by MRE, (2) size of the HCCs, (3) number of HCCs, and (4) presence of HBP hypointense nodule without APHE. Pathological findings included tumour grade, vascular/biliary/capsule invasion, and fibrosis stage of the liver. Considering imaging/pathological findings and patients' characteristics as dependent variables, Cox proportional hazards model analysis was performed to identify independent factors associated with late recurrence after surgery.

RESULTS: The median follow-up period was 37.3 months. During follow-up, 29 patients (32.5%) developed late recurrence after surgery. In multivariate analysis, underlying liver disease (viral hepatitis) and presence of HBP hypointense nodules without APHE (p=0.010 and 0.033, respectively) were independently associated with disease-free survival (DFS). Kaplan–Meier analysis revealed that patients with HBP hypointense nodules without APHE had a significantly lower DFS rate than those without the nodule (39.2% versus 74.1% at 3 years after surgery, p=0.008).

CONCLUSION: The presence of HBP hypointense nodules without APHE was an indicator of late recurrence after surgery for HCC.

* Guarantor and correspondent: S. Ichikawa, Department of Radiology, University of Yamanashi, 1110 Shimokato, Chuo-shi, Yamanashi, 409-3898, Japan. Tel.: +81-55-273-1111; fax: +81-55-273-6744.
E-mail address: sichikawa@yamanashi.ac.jp (S. Ichikawa).

https://doi.org/10.1016/j.crad.2019.08.002
0009-9260/

Introduction

Hepatocellular carcinoma (HCC) is the most common form of primary liver cancer. Current treatment options for HCC are radiofrequency ablation, curative resection, and transplantation.[1] Repeated surgery is performed for selected cases only because most patients with HCC also have liver dysfunction or other medical conditions that could cause surgical complications. There are two types of recurrence after radiofrequency ablation or curative resection of HCC: (1) intrahepatic metastasis and (2) multicentric recurrence.[2] Intrahepatic metastasis is defined as metastasis originating from the treated HCC via the intrahepatic portal vein that was not detected at the time of treatment because of its small size. Retrospective genetic analyses of HCC revealed that intrahepatic metastasis tends to occur early after surgery, whereas multicentric recurrence usually occurs at a later stage.[3] The risk of intrahepatic metastasis depends on the tumour characteristics, such as tumour grade, micro- and macrovascular invasion, and presence of satellite nodules.[1,4] Multicentric recurrence is characterized by metachronous hepatocarcinogenesis in the remnant liver, and it typically occurs independently from the treated HCC. The risk of multicentric recurrence depends on the risk of hepatocarcinogenesis of the liver.[5] Distinguishing these two types of recurrence is important for determining treatment. Intrahepatic metastasis suggests that the treatment for HCC was not effective, and that tumour cells could have already spread to the blood. Multicentric recurrence suggests a newly developed HCC that is unrelated to the former HCC, and thus, can be treated by radiofrequency ablation or resection. The prognosis of patients with multicentric recurrence is significantly better than that of patients with intrahepatic metastasis.[6]

A hepatobiliary phase (HBP) hypointense hepatocellular nodule without arterial phase hyperenhancement (APHE)[7] is detected as a hypointense signal in the HBP after injection of a hepatobiliary contrast agent in patients with cirrhosis (Fig 1). This nodule has been of great interest among researchers in the fields of hepatology and radiology because it might represent a transition from a benign hepatocellular nodule to HCC.[8,9] Recent reports have shown that patients with HBP hypointense nodules without APHE are at high risk of development of progressed HCC, including HCC with hypervascularity[10–12] and the development of HCC elsewhere in the liver.[13,14] Therefore, a HBP hypointense nodule without APHE is considered a predictor of multicentric recurrence after treatment for HCC.[15]

Magnetic resonance elastography (MRE) is a non-invasive method of measuring liver stiffness that is widely used for staging liver fibrosis in the clinical setting. High liver stiffness measured at MRE suggests cirrhosis, a risk factor for HCC development.[16,17] It has been reported that the presence of both a HBP hypointense nodule without APHE and high liver stiffness increase the likelihood of HCC recurrence or poor prognosis after resection of a progressed HCC[15,18]; however, it is not clear which is the predominant risk factor predicting multicentric recurrence. Therefore, the purpose of this study was to evaluate the value of magnetic resonance imaging (MRI) features, including liver stiffness measured by MRE and the presence of HBP hypointense nodule without APHE, for predicting late recurrence (>1 year) after surgery for HCC.

Materials and methods

Patients

This retrospective study followed the principles of the Declaration of Helsinki and was approved by the institutional review board. The requirement for written informed consent from the patients was waived because of the retrospective design of the study.

This study included 124 patients who underwent surgical resection for HCC at Fujiyoshida Municipal Medical Center between February 2010 and April 2015. Patient data were retrieved from electronic patient charts (databases). Exclusion criteria were: (1) a follow-up period <1 year (n=8) and (2) early recurrence (within 1 year) after surgical resection (n=27; Fig 2). All patients underwent gadoxetate disodium-enhanced MRI within 5 months before surgery. Finally, 89 patients (69 men and 20 women) aged 46–89 years (mean, 69.3±8.7 years) were included in the analysis. Of those, 46 patients had chronic hepatitis C, 15 had chronic hepatitis B, 17 had alcoholic hepatitis, and 11 had other aetiology of liver disease, namely non-alcoholic steatohepatitis (n=1), primary biliary cholangitis (n=1), and uncertain liver disease with elevated liver enzyme levels (n=9).

MRI

Gadoxetate disodium-enhanced MRI was performed in all patients using either a 1.5 T MRI system with a superconducting magnet (Signa Excite HD, GE Healthcare, Waukesha, WI, USA) with an eight-channel phased-array coil or a 3 T MRI system (Discovery 750, GE Healthcare, Waukesha, WI, USA) with a 32-channel phased-array coil.

Dynamic fat-saturated T1-weighted gradient-echo images were obtained with a three-dimensional (3D) acquisition sequence (liver acquisition with volume acceleration [LAVA]) before and 20–30 seconds (arterial phase with fluoroscopic triggering technique), 60 seconds (portal venous phase), 2 minutes (late phase), and 20 minutes (HBP) after the administration of gadoxetate disodium. The contrast material was administered intravenously as a bolus (0.025 mmol/kg of body weight) at a rate of 1 ml/s flushed with 20 ml of saline using a power injector. The scan timing was adjusted using the fluoroscopic triggering technique. Arterial and hepatobiliary phase images were used for analysis. The images were acquired in the axial plane and had a section thickness of 5 mm and a 2.5-mm overlap (i.e., 2.5-mm interval). Table 1 summarizes the MRI sequence parameters of arterial and hepatobiliary phase imaging. One radiologist (M.M.) with 1 year of experience in liver

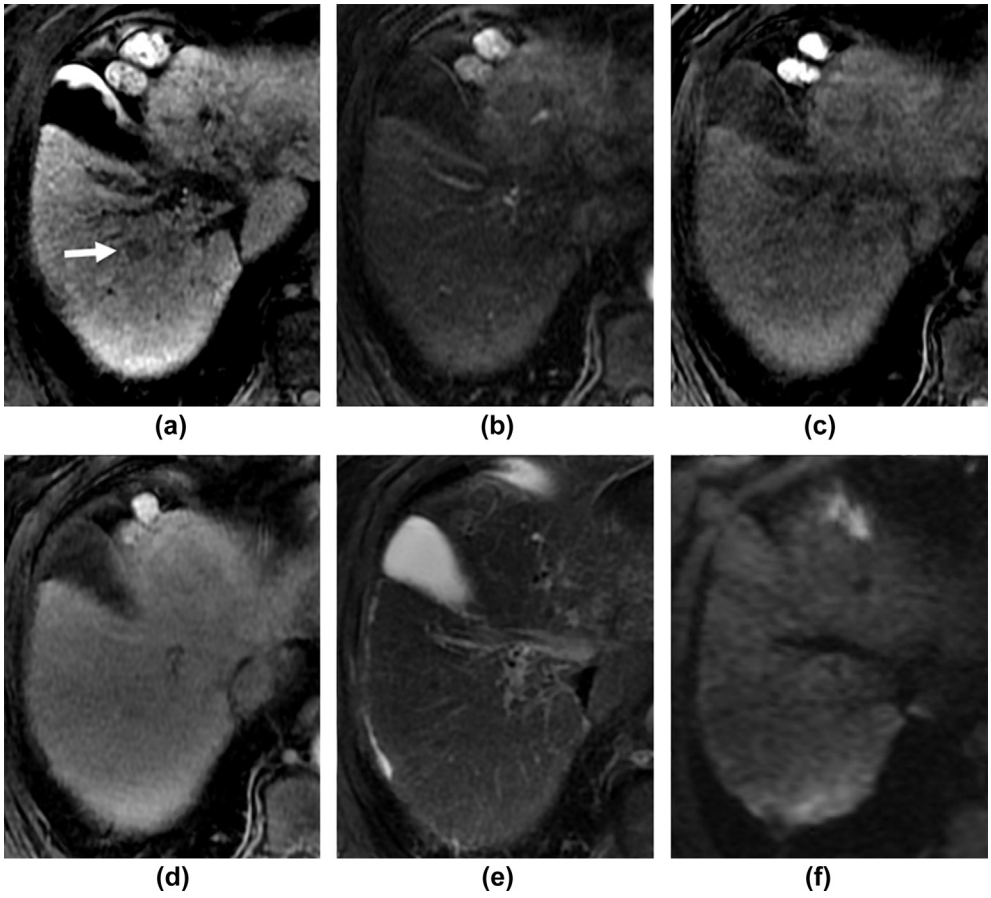

Figure 1 Imaging findings of a 66-year-old man with a HBP hypointense nodule without APHE. (a) HBP; (b) arterial phase; (c) precontrast image; (d) portal venous phase; (e) fat-suppression T2-weighted image; (f) diffusion-weighted image (b-value=1,000 s/mm^2). (a) The HBP image shows a hypointense nodule of 8 mm in diameter at S7/8 (arrow). (b) The arterial phase image does not show hyperenhancement. (c–f) The nodule could not be detected in other phases.

MRI evaluated the following findings for HCC under the supervision of a board-certificated radiologist (U.M., with 17 years of experience in liver MRI): size (the greatest transverse diameter on axial images), number of tumours (solitary or multiple), uptake of gadoxetate disodium (absent or present), and HBP hypointense nodule without APHE (absent or present).

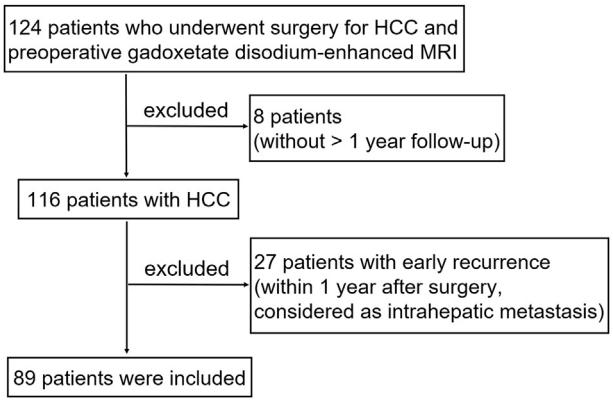

Figure 2 Inclusion criteria for patient enrollment. Patients with early recurrence (within 1 year) after surgery were excluded from this study as they were assumed to have intrahepatic metastasis.

MRE

MRE was also performed using either a 1.5 or 3 T MRI system. Patients were placed in the supine position, and

Table 1
Sequence parameters of arterial phase and hepatobiliary phase image.

	Arterial phase		Hepatobiliary phase	
	1.5 T	3T	1.5 T	3 T
Sequence	3D-GRE T1WI (LAVA)	3D-GRE T1WI (LAVA)	3D-GRE T1WI (LAVA)	3D-GRE T1WI (LAVA)
Repetition time/echo time (ms)	4.8/1.9	4.8/2.0	3.8/1.9	3.0/1.4
Matrix	320 × 192	320 × 192	320 × 192	256 × 192
Field of view (cm)	35–42 × 40–45	34 × 27.2	35–42 × 40–45	34 × 27.2
Section thickness/ intersection gap (mm)	5/2.5	5/2.5	5/2.5	5/2.5
Number of signals acquired	1	1	1	1
Flip angle (degree)	15	15	12	12
Scan delay after injection	20–30 s	20–30 s	20 min	20 min

Abbreviation: 3D, 3-dimentional; GRE, gradient echo; T1WI, T1-weighte imaging; LAVA, liver acquisition with volume acceleration.

a cylindrical passive driver was attached to the right chest wall using a rubber belt. A pneumatic vibration was delivered through a plastic cylinder from a vibrator placed outside the imaging room to the passive driver. The scanning position was above the gallbladder and below the subphrenic region of the liver. Patients were instructed to hold their breath after expiration to maintain a consistent position during image acquisition at each phase offset. Table 2 summarizes the parameters of MRE. The MRI systems automatically generated liver stiffness maps by processing the acquired propagating shear-wave images according to a two-dimensional (2D) inversion algorithm, and shear stiffness of the tissue was translated to a pixel value (kPa). The placement of regions of interest for measurement of liver stiffness was performed by a board-certificated radiologist (S.I., with 10 years of experience in liver MRI) with careful attention to avoid heterogeneous wave propagation in the right lobe of the liver of each patient. Regions of interest of at least 1.5 cm^2 were placed to exclude blood vessels seen on a magnitude image of MRE and the edge of the liver and to include a parallel wave form without interference on the phase images.

Follow-up and diagnosis of late recurrence

All patients were followed up at the outpatient clinic with blood tests, including tumour markers, and imaging examinations, including abdominal ultrasound, dynamic contrast-enhanced computed tomography, and MRI. A radiologist (M.M.) reviewed all the images and radiological reports to find recurrence under the supervision of a board-certified radiologist (U.M.). The diagnostic criteria of recurrence were APHE and washout without taking nodule size into account, as proposed by the Japanese Society of Hepatology. In this study, a non-hypervascular nodule was not considered a sign of recurrence, and late recurrence was defined as a recurrent event occurring >1 year after surgical resection.

Statistical analysis

Cox proportional hazard model was used to identify independent factors associated with late recurrence (disease-free survival and overall survival), including preoperative patient characteristics (age, sex, underlying liver disease [viral hepatitis versus non-viral hepatitis], and history of HCC), blood test findings (alpha-fetoprotein, protein induced by vitamin K absence-II, albumin, lactate dehydrogenase, aspartate transaminase, alanine aminotransferase, leucine aminopeptidase, alkaline phosphatase, gamma-glutamyl transpeptidase, total bilirubin, prothrombin time, platelet count, and indocyanine green retention test after 15 minutes), imaging findings (tumour size, number, liver stiffness measured by MRE, and the presence of HBP hypointense nodule without APHE), and pathological findings (fibrosis score, tumour grade, portal vein invasion, hepatic vein invasion, and infiltration to the capsule). Univariate analyses were performed to determine the variables associated with late recurrence (disease-free survival and overall survival). Variables showing a p-value <0.10 in univariate analysis were subjected to multivariate Cox proportional

Table 2
Sequence parameters of magnetic resonance elastography.

	1.5 T	3 T
Sequence	2D-GRE	2D-GRE
Plane	Transverse	Transverse
Repetition time/echo time, ms	100/27	50/20
Matrix	256 × 64	256 × 80
Field of view, cm	36 × 27	35 × 35
Section thickness/intersection gap, mm	10/5	10/5
Number of signals acquired	1	1
Flip angle	30°	23°
Acquisition time, s	13	17
Frequency of driver, Hz	60	60
Amplitude, %	60	70
Axis of motion-sensitizing gradient pulse	z	z

2D, two-dimensional; GRE, gradient echo.

Table 3
Demographic data for 89 patients.

Variables	
Clinical data	
Age, years	70 (46–89)
Sex, M/F	69/20
Follow-up period, months	37.3 (12–74.9)
Underlying liver disease: hepatitis C/hepatitis B/alcohol/other	46/15/17/11
History of hepatocellular carcinoma: absent/present	67/22
Alpha-fetoprotein, nmol/l	2.6 (0.56–6437)
Protein induced by vitamin K absence-II, AU/l	21 (8–17483)
Albumin, g/l	40 (21–49)
Lactate dehydrogenase, IU/l	189.5 (113–342)
Aspartate aminotransferase, IU/l	33 (13–149)
Alanine aminotransferase, IU/l	33 (9–168)
Leukocyte alkaline phosphatase, U/l	56 (33–251)
Alkaline phosphatase, IU/l	275.5 (122–713)
Gamma-glutamyl transferase, IU/l	43.5 (12–359)
Total bilirubin, ìmol/l	12 (5.1–32.5)
Prothrombin time, %	84.6 (50–117.4)
Platelet count, 10^9/l	13.9×10^7 (5.8×10^7 –33.5×10^7)
Indocyanine green retention test after 15 min (ICG R15), %	13.9 (4.3–34.3)
Child–Pugh class: A/B	81/8
Imaging findings	
Size of tumour, mm	24.5 (6–130)
Number of tumours: solitary/multiple	60/29
Uptake of gadoxetic acid: absent/present	79/10
Liver stiffness by magnetic resonance elastography, kPa	3.4 (1.6–9)
HBP hypointense nodule without APHE: absent/present	66/23
Pathological findings	
Fibrosis, F1/F2/F3/F4	11/21/26/31
Tumour grade: low–moderate/high	71/18
Portal vein invasion: absent/present	75/14
Hepatic vein invasion: absent/present	80/9
Hepatic artery invasion: absent/present	89/0
Bile duct invasion: absent/present	88/1
Infiltration to the capsule: absent/present	33/56

Continuous variables were expressed as median (range).
HBP, hepatobiliary phase; APHE, arterial phase hyperenhancement

Table 4
Univariate and multivariate analyses for disease-free survival with Cox proportional hazards model.

Variables	Univariate analysis			Multivariate analysis		
	Risk ratio	95% CI	*p*-Value	Risk ratio	95% CI	*p*-Value
Clinical data						
Age	0.994	0.958–1.033	0.765			
Sex (man versus woman)	2.195	0.665–7.249	0.197			
Underlying liver disease (viral hepatitis versus non-viral hepatitis)	2.459	1.189–5.087	0.015[a]	2.767	1.280–5.981	0.010[a]
History of hepatocellular carcinoma (present versus absent)	1.855	0.880–3.910	0.105			
Alpha-fetoprotein	1.000	0.999–1.000	0.909			
Protein induced by vitamin K absence-II	1.000	0.999–1.000	0.406			
Albumin	1.135	0.522–2.748	0.766			
Lactate dehydrogenase	1.008	0.999–1.017	0.077[b]	1.008	0.999–1.017	0.063
Aspartate aminotransferase	0.999	0.977–1.016	0.884			
Alanine aminotransferase	1.001	0.982–1.015	0.930			
Leukocyte alkaline phosphatase	1.002	0.985–1.013	0.722			
Alkaline phosphatase	0.999	0.996–1.003	0.729			
Gamma-glutamyl transferase	1.000	0.991–1.007	0.996			
Total bilirubin	0.985	0.202–4.005	0.984			
Prothrombin time	1.008	0.980–1.038	0.580			
Platelet count	1.017	0.943–1.088	0.640			
Indocyanine green retention test after 15 min	1.005	0.942–1.067	0.873			
Child–Pugh class (B versus A)	0.993	0.300–3.282	0.991			
Imaging findings						
Size of tumour	1.003	0.984–1.016	0.748			
Number of tumours (multiple versus solitary)	1.585	0.761–3.299	0.218			
Uptake of gadoxetic acid (present versus absent)	1.565	0.541–4.527	0.408			
Liver stiffness by magnetic resonance elastography	1.164	0.910–1.469	0.211			
HBP hypointense nodule without APHE (present versus absent)	2.570	1.244–5.301	0.011[a]	2.272	1.066–4.839	0.033[a]
Pathological findings						
Severe fibrosis (F3–4 versus F0–2)	1.986	0.843–4.679	0.117			
Tumour grade (high versus others)	1.361	0.520–3.562	0.531			
Portal vein invasion (present versus absent)	1.018	0.388–2.672	0.972			
Hepatic vein invasion (present versus absent)	1.664	0.577–4.795	0.346			
Infiltration to the capsule (present versus absent)	1.651	0.793–3.439	0.180			

[a] $p<0.05$.
[b] $p<0.10$.
HBP, hepatobiliary phase; APHE, arterial phase hyperenhancement; CI, confidence interval.

hazards regression analysis. The Kaplan–Meier method was used to calculate the disease-free survival rate using the log-rank test. Differences with a *p*-value <0.05 were considered to be significant. All statistical analyses were performed using JMP software (version 14.1.0; SAS Institute, Cary, NC, USA).

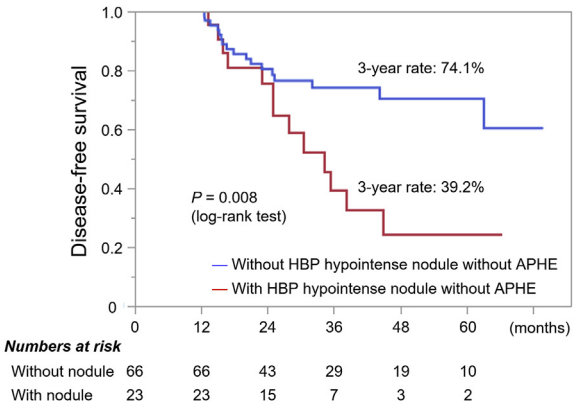

Figure 3 Disease-free survival in patients with resected HCC. Kaplan–Meier analysis revealed that disease-free survival was significantly different according to the presence or absence of a HBP hypointense nodule without APHE (p=0.008).

Results

Characteristics of the patients and nodules

HBP hypointense nodule without APHE was found in 22 of the 89 patients (24.7%). The median follow-up period was 37.3 months (range, 12–74.9 months). During the follow-up period, 29 patients (32.5%) developed late recurrence after surgical resection. Of the 29 patients, six (20.7%) had recurrence originating from the HBP hypointense nodule without APHE, namely, from a hypervascularized HBP hypointense nodule without APHE. The remaining 23 patients (79.3%) had recurrence in the region where no nodule was detected on preoperative gadoxetate disodium-enhanced MRI (imaging-occult carcinogenesis[19] or rapidly progressing hepatocarcinogenesis). In six out of 22 cases (27.3%), the HBP hypointense nodule without APHE became hypervascular HCC during the follow-up period. Late recurrence occurred more frequently in patients with a HBP hypointense nodule without APHE (12/22 [54.5%]) than in patients without a HBP hypointense nodule without APHE (17/67 [25.3%]; p=0.011). Four patients (4.5%) died of HCC recurrence (n=2), other cause (brain haemorrhage, n=1), or unknown cause (n=1).

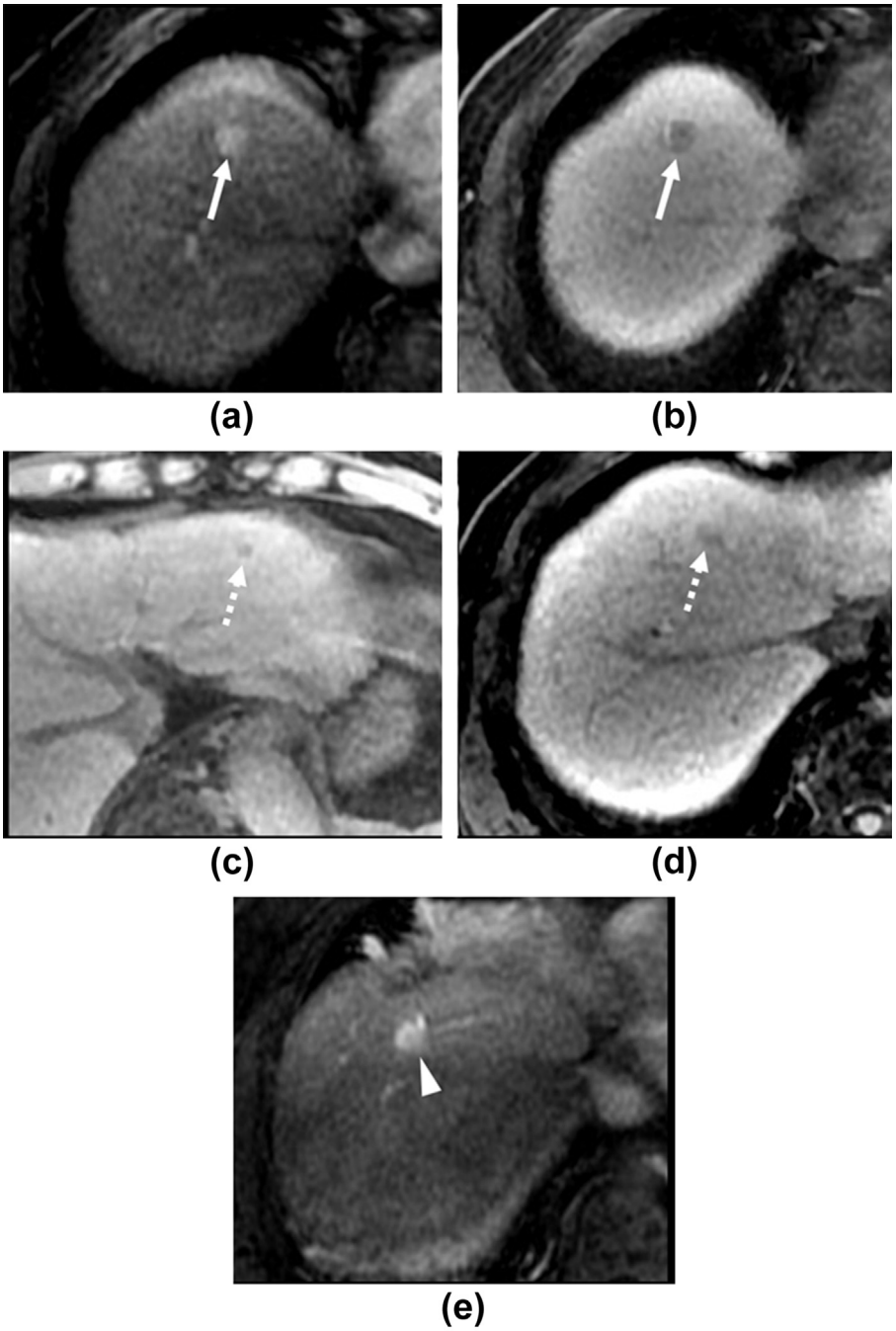

Figure 4 A case of small HCC with a HBP hypointense nodule without APHE that developed late recurrence. A 74-year-old man had a small hypervascular HCC (10 mm) at S8 (a, b, arrows). (c,d) Preoperative MRI images revealed HBP hypointense nodules without APHE (dashed arrows) in the liver. (e) One of the HBP hypointense nodules without APHE became a hypervascular HCC (arrowhead) 17 months after surgery (multicentric recurrence).

Table 3 summarizes the demographic data of the 89 patients.

Risk factors for late recurrence

Univariate analyses revealed that the risk factors for late recurrence were underlying liver disease (viral hepatitis), lactate dehydrogenase level, and the presence of HBP hypointense nodule without APHE (p=0.011–0.077). Whereas liver stiffness measured by MRE was not an independent predictor for late recurrence (p=0.211). Multivariate logistic regression analysis with these variables revealed that underlying liver disease (viral hepatitis; risk ratio [RR], 2.767; 95% confidence interval [CI], 1.280–5.981; p=0.010) and the presence of a HBP hypointense nodule without APHE (RR, 2.272; 95% CI, 1.066–4.839; p=0.033) were the independent risk factors for late recurrence (disease-free survival, Table 4).

Disease-free survival

The results of Kaplan–Meier analysis revealed that patients with HBP hypointense nodule without APHE had a significantly lower disease-free survival rate than those without HBP hypointense nodule without APHE 39.2% versus 74.1% at 3 years after hepatectomy (p=0.008, Fig 3). Fig. 4 shows a case of a patient with a small HCC and a HBP hypointense nodule without APHE who presented with late recurrence after surgery.

Overall survival

Univariate analyses revealed that the risk factors for overall survival included female sex (p=0.034) and hepatic vein invasion (p=0.059). Whereas liver stiffness measured by MRE was not an independent predictor for overall survival (p=0.698). Multivariate logistic regression analysis with these variables revealed that female sex (RR, 7.870; 95% CI, 1.382–44.82; p=0.020) and hepatic vein invasion (RR, 7.684; 95% CI, 1.222–48.32; p=0.030) were the independent risk factors for overall survival (Table 5).

Discussion

The present study demonstrated a higher rate of late recurrence, or multicentric recurrence in most cases, of HCC in patients with a HBP hypointense nodule without APHE than in patients without a nodule. There was no significant difference in overall survival between the two

Table 5
Univariate and multivariate analyses for overall survival with Cox proportional hazards model.

Variables	Univariate analysis			Multivariate analysis		
	Risk ratio	95% CI	p-Value	Risk ratio	95% CI	p-Value
Clinical data						
Age	1.038	0.948–1.145	0.431			
Sex (woman versus man)	5.749	1.145–28.86	0.034[a]	7.870	1.382–44.82	0.020[a]
Underlying liver disease (viral hepatitis versus non-viral hepatitis)	1.565	0.256–9.549	0.628			
History of hepatocellular carcinoma (present versus absent)	2.401	0.483–12.01	0.284			
Alpha-fetoprotein	0.994	0.949–1.000	0.635			
Protein induced by vitamin K absence-II	1.000	0.997–1.000	0.616			
Albumin	0.586	0.143–4.106	0.531			
Lactate dehydrogenase	1.003	0.982–1.021	0.802			
Aspartate aminotransferase	0.954	0.858–1.021	0.278			
Alanine aminotransferase	0.990	0.927–1.035	0.710			
Leukocyte alkaline phosphatase	1.008	0.947–1.051	0.771			
Alkaline phosphatase	0.999	0.991–1.006	0.753			
Gamma-glutamyl transferase	1.003	0.981–1.021	0.795			
Total bilirubin	0.396	0.004–16.70	0.662			
Prothrombin time	1.005	0.944–1.072	0.995			
Platelet count	1.038	0.873–1.201	0.654			
Indocyanine green retention test after 15 min	1.084	0.916–1.265	0.320			
Child–Pugh class (B vs A)	4.772×10^{-9}	0–NA	0.999			
Imaging findings						
Size of tumour	1.012	0.978–1.035	0.370			
Number of tumours (multiple versus solitary)	1.202	0.219–6.611	0.833			
Uptake of gadoxetic acid (present versus absent)	4.872×10^{-9}	0–NA	0.999			
Liver stiffness by magnetic resonance elastography	0.891	0.444–1.487	0.698			
HBP hypointense nodule without APHE (present versus absent)	1.273×10^{-9}	0–NA	0.999			
Pathological findings						
Severe fibrosis (F3–4 versus F0–2)	0.701	0.140–3.506	0.665			
Tumour grade (high versus others)	3.318	0.668–16.49	0.143			
Portal vein invasion (present versus absent)	2.384	0.429–13.24	0.321			
Hepatic vein invasion (present versus absent)	5.189	0.940–28.66	0.059[b]	7.684	1.222–48.32	0.030[a]
Infiltration to the capsule (present versus absent)	3.609	0.654–19.93	0.141			

[a] $p<0.05$.
[b] $p<0.10$.
HBP, hepatobiliary phase; APHE, arterial phase hyperenhancement; CI, confidence interval; NA, not available.

groups, probably because of the small sample size. From the present results, patients might not die soon after late recurrence when primary HCC was resected. This may because treatment for recurrence (e.g., reoperation, transarterial chemoembolization, or radiofrequency ablation) is effective.

Previous studies have suggested that the presence of a HBP hypointense nodule without APHE was an independent risk factor of recurrence after surgery[15] or radiofrequency ablation,[20–22] which is consistent with the present findings. An HBP hypointense nodule without APHE is considered a high-risk hepatocellular nodule in the course of multistep hepatocarcinogenesis, which includes early HCC or high-grade dysplastic nodules[23,24] and progression to hypervascular HCC in patients with cirrhosis. The present results showed that 20.7% (6/29) of cases of late recurrence originated from a HBP hypointense nodule without APHE, namely from a hypervascularized HBP hypointense nodule without APHE, whereas the remaining 79.3% (23/29) cases of late recurrence originated from the region where no nodule was detected on preoperative gadoxetate disodium-enhanced MRI (imaging-occult carcinogenesis[19] or rapidly progressing hepatocarcinogenesis). Considering all of these observations, a HBP hypointense nodule without APHE was considered a sign of accelerated hepatocarcinogenesis in the entire liver, rather than a simple precursor of hypervascular HCC. It is important to determine the presence of HBP hypointense nodules without APHE on HBP images to help decision-making in patients with HCC (e.g., to recommend frequent imaging follow-up to detect small-sized hypervascular HCCs). Liver screening tests including HBP images could help identify recurrent HCC at early stages and improve the prognosis of patients with chronic liver disease.[25]

Liver stiffness is another known risk factor for HCC recurrence[26]; however, in the present study, liver stiffness measured by MRE was not independently associated with late recurrence of HCC. In MRE, liver stiffness varies not only by fibrosis stage, but also by type of underlying liver disease[27–30] and degree of inflammation.[31,32] These variations might be confounding factors in the present study. The difference between previous study[26] and current data is that the previous study was focused on early HCC recurrence whereas the present study was focused on late HCC recurrence. It might influence the result, however further studies are needed in order to clarify MRE can found to a risk of HCC recurrence or not. It is also interesting to note that in the present study, the presence of a HBP hypointense nodule without APHE was a stronger indicator of late recurrence than were pathological findings of liver fibrosis. The signal intensities in HBP might more directly indicate the stage of hepatocarcinogenesis than fibrosis.

The present study has some limitations. First, the major limitation of the present study is its retrospective design. Second, there is the possibility of selection bias because of the indication for surgery. Third, the aetiology of liver disease varied widely, and the risk of hepatocarcinogenesis is known to depend on the aetiology of liver disease.[33] Further studies with a homogeneous sample and a prospective study design are warranted to confirm the present findings.

In conclusion, the presence of a HBP hypointense nodule without APHE is an indicator of late recurrence (>1 year) after surgery for HCC.

Conflict of interest

The authors declare no conflict of interest.

References

1. Tabrizian P, Jibara G, Shrager B, *et al*. Recurrence of hepatocellular cancer after resection: patterns, treatments, and prognosis. *Ann Surg* 2015;**261**:947–55.
2. Kumada T, Nakano S, Takeda I, *et al*. Patterns of recurrence after initial treatment in patients with small hepatocellular carcinoma. *Hepatology* 1997;**25**:87–92.
3. Finkelstein SD, Marsh W, Demetris AJ, *et al*. Microdissection-based allelotyping discriminates de novo tumour from intrahepatic spread in hepatocellular carcinoma. *Hepatology* 2003;**37**:871–9.
4. Muhi A, Ichikawa T, Motosugi U, *et al*. Diffusion-weighted imaging of hepatocellular carcinoma for predicting early recurrence and survival after hepatectomy. *Hepatol Int* 2013;**7**:662–8.
5. Nomoto S, Hishida M, Inokawa Y, *et al*. Management of hepatocellular carcinoma should consider both tumour factors and background liver factors. *Hepatobiliary Surg Nutr* 2014;**3**:82–5.
6. Yang SL, Luo YY, Chen M, *et al*. A systematic review and meta-analysis comparing the prognosis of multicentric occurrence and versus intrahepatic metastasis in patients with recurrent hepatocellular carcinoma after hepatectomy. *HPB (Oxford)* 2017;**19**:835–42.
7. Motosugi U, Murakami T, Lee JM, *et al*. Recommendation for terminology: nodules without arterial phase hyperenhancement and with hepatobiliary phase hypointensity in chronic liver disease. *J Magn Reson Imaging* 2018;**48**:1169–71.
8. Motosugi U, Bannas P, Sano K, *et al*. Hepatobiliary MR contrast agents in hypovascular hepatocellular carcinoma. *J Magn Reson Imaging* 2015;**41**:251–65.
9. Van Beers BE, Pastor CM, Hussain HK. Primovist, eovist: what to expect? *J Hepatol* 2012;**57**:421–9.
10. Kumada T, Toyoda H, Tada T, *et al*. Evolution of hypointense hepatocellular nodules observed only in the hepatobiliary phase of gadoxetate disodium-enhanced MRI. *AJR Am J Roentgenol* 2011;**197**:58–63.
11. Motosugi U, Ichikawa T, Sano K, *et al*. Outcome of hypovascular hepatic nodules revealing no gadoxetic acid uptake in patients with chronic liver disease. *J Magn Reson Imaging* 2011;**34**:88–94.
12. Hyodo T, Murakami T, Imai Y, *et al*. Hypovascular nodules in patients with chronic liver disease: risk factors for development of hypervascular hepatocellular carcinoma. *Radiology* 2013;**266**:480–90.
13. Komatsu N, Motosugi U, Maekawa S, *et al*. Hepatocellular carcinoma risk assessment using gadoxetic acid-enhanced hepatocyte phase magnetic resonance imaging. *Hepatol Res* 2014;**44**:1339–46.
14. Ichikawa S, Ichikawa T, Motosugi U, *et al*. Presence of a hypovascular hepatic nodule showing hypointensity on hepatocyte-phase image is a risk factor for hypervascular hepatocellular carcinoma. *J Magn Reson Imaging* 2014;**39**:293–7.
15. Toyoda H, Kumada T, Tada T, *et al*. Non-hypervascular hypointense nodules detected by Gd-EOB-DTPA-enhanced MRI are a risk factor for recurrence of HCC after hepatectomy. *J Hepatol* 2013;**58**:1174–80.
16. Ichikawa S, Motosugi U, Enomoto N, *et al*. Magnetic resonance elastography can predict development of hepatocellular carcinoma with longitudinally acquired two-point data. *Eur Radiol* 2019;**29**:1013–21.
17. Motosugi U, Ichikawa T, Koshiishi T, *et al*. Liver stiffness measured by magnetic resonance elastography as a risk factor for hepatocellular carcinoma: a preliminary case-control study. *Eur Radiol* 2013;**23**:156–62.
18. Lee DH, Lee JM, Yi NJ, *et al*. Hepatic stiffness measurement by using MR elastography: prognostic values after hepatic resection for hepatocellular carcinoma. *Eur Radiol* 2017;**27**:1713–21.

19. Ichikawa S, Ichikawa T, Motosugi U, *et al*. Was hypervascular hepatocellular carcinoma visible on previous gadoxetic acid-enhanced magnetic resonance images? *Liver Cancer* 2015;**4**:154–62.
20. Iwamoto T, Imai Y, Igura T, *et al*. Non-hypervascular hypointense hepatic nodules during the hepatobiliary phase of gadolinium-ethoxybenzyl-diethylenetriamine pentaacetic acid-enhanced MRI as a risk factor of intrahepatic distant recurrence after radiofrequency ablation of hepatocellular carcinoma. *Dig Dis* 2017;**35**:574–82.
21. Inoue M, Ogasawara S, Chiba T, *et al*. Presence of non-hypervascular hypointense nodules on gadolinium-ethoxybenzyl-diethylenetriamine pentaacetic acid-enhanced magnetic resonance imaging in patients with hepatocellular carcinoma. *J Gastroenterol Hepatol* 2017;**32**:908–15.
22. Lee DH, Lee JM, Lee JY, *et al*. Non-hypervascular hepatobiliary phase hypointense nodules on gadoxetic acid-enhanced MRI: risk of HCC recurrence after radiofrequency ablation. *J Hepatol* 2015;**62**:1122–30.
23. Kobayashi S, Matsui O, Gabata T, *et al*. Intranodular signal intensity analysis of hypovascular high-risk borderline lesions of HCC that illustrate multi-step hepatocarcinogenesis within the nodule on Gd-EOB-DTPA-enhanced MRI. *Eur J Radiol* 2012;**81**:3839–45.
24. Kitao A, Matsui O, Yoneda N, *et al*. The uptake transporter OATP8 expression decreases during multistep hepatocarcinogenesis: correlation with gadoxetic acid enhanced MR imaging. *Eur Radiol* 2011;**21**:2056–66.
25. Wen T, Jin C, Facciorusso A, *et al*. Multidisciplinary management of recurrent and metastatic hepatocellular carcinoma after resection: an international expert consensus. *Hepatobiliary Surg Nutr* 2018;**7**:353–71.
26. Wang J, Shan Q, Liu Y, *et al*. 3D MR elastography of hepatocellular carcinomas as a potential biomarker for predicting tumour recurrence. *J Magn Reson Imaging* 2019;**49**:719–30.
27. Ichikawa S, Motosugi U, Ichikawa T, *et al*. Magnetic resonance elastography for staging liver fibrosis in chronic hepatitis C. *Magn Reson Med Sci* 2012;**11**:291–7.
28. Ichikawa S, Motosugi U, Morisaka H, *et al*. Validity and reliability of magnetic resonance elastography for staging hepatic fibrosis in patients with chronic hepatitis B. *Magn Reson Med Sci* 2015;**14**:211–21.
29. Chen J, Talwalkar JA, Yin M, *et al*. Early detection of nonalcoholic steatohepatitis in patients with nonalcoholic fatty liver disease by using MR elastography. *Radiology* 2011;**259**:749–56.
30. Jhaveri KS, Hosseini-Nik H, Sadoughi N, *et al*. The development and validation of magnetic resonance elastography for fibrosis staging in primary sclerosing cholangitis. *Eur Radiol* 2019;**29**:1039–47.
31. Ichikawa S, Motosugi U, Nakazawa T, *et al*. Hepatitis activity should be considered a confounder of liver stiffness measured with MR elastography. *J Magn Reson Imaging* 2015;**41**:1203–8.
32. Yoshimitsu K, Mitsufuji T, Shinagawa Y, *et al*. MR elastography of the liver at 3.0 T in diagnosing liver fibrosis grades; preliminary clinical experience. *Eur Radiol* 2016;**26**:656–63.
33. Yamamoto T, Kajino K, Kudo M, *et al*. Determination of the clonal origin of multiple human hepatocellular carcinomas by cloning and polymerase chain reaction of the integrated hepatitis B virus DNA. *Hepatology* 1999;**29**:1446–52.